Systems/Circuits

Synaptic Adaptations at the Rostromedial Tegmental Nucleus Underlie Individual Differences in Cocaine Avoidance Behavior

Jeffrey Parrilla-Carrero,[1*] Maya Eid,[1*] Hao Li,[2] Ying S. Chao,[1] and Thomas C. Jhou[1]
[1]Department of Neurosciences, Medical University of South Carolina, Charleston, South Carolina 29425, and [2]Salk Institute for Biological Studies, La Jolla, California 92037

Although cocaine is powerfully rewarding, not all individuals are equally prone to abusing this drug. We postulate that these differences arise in part because some individuals exhibit stronger aversive responses to cocaine that protect them from cocaine seeking. Indeed, using conditioned place preference (CPP) and a runway operant cocaine self-administration task, we demonstrate that avoidance responses to cocaine vary greatly between individual high cocaine-avoider and low cocaine-avoider rats. These behavioral differences correlated with cocaine-induced activation of the rostromedial tegmental nucleus (RMTg), measured using both *in vivo* firing and c-*fos*, whereas slice electrophysiological recordings from ventral tegmental area (VTA)-projecting RMTg neurons showed that relative to low avoiders, high avoiders exhibited greater intrinsic excitability, greater transmission via calcium-permeable AMPA receptors (CP-AMPARs), and higher presynaptic glutamate release. In behaving animals, blocking CP-AMPARs in the RMTg with NASPM reduced cocaine avoidance. Hence, cocaine addiction vulnerability may be linked to multiple coordinated synaptic differences in VTA-projecting RMTg neurons.

Key words: CP-AMPA; CP-AMPAR; RMTg; runway

Significance Statement

Although cocaine is highly addictive, not all individuals exposed to cocaine progress to chronic use for reasons that remain unclear. We find that cocaine's aversive effects, although less widely studied than its rewarding effects, show more individual variability, are predictive of subsequent propensity to seek cocaine, and are driven by variations in RMTg in response to cocaine that arise from distinct alterations in intrinsic excitability and glutamate transmission onto VTA-projecting RMTg neurons.

Introduction

Although drugs of abuse are powerfully rewarding, not all individuals exposed to them are equally prone to developing substance use disorder (Tsuang et al., 1998; Van Etten and Anthony, 1999; Deroche-Gamonet et al., 2004; Ellenbroek et al., 2005). The reasons for these differences are not known but may involve neurobiological substrates whose elucidation could lead to improved therapies to treat or event prevent addiction.

Individual differences in vulnerability to drug abuse may arise from predisposing factors that exist even before the first drug experience (Uhl, 2004; Koob, 2006; Sweitzer et al., 2012). One such predisposing factor is behavioral sensitivity to the acute aversive attributes of abused drugs, which influences seeking of morphine, cocaine, nicotine, and alcohol (Koob and Le Moal, 2008; Wheeler et al., 2008, 2015; Ettenberg, 2009; Davis and Riley, 2010; Riley, 2011; Piazza and Deroche-Gamonet, 2013; Fowler and Kenny, 2014). Furthermore, we and others have also found that psychomotor stimulants, such as cocaine, produce aversive conditioning reactions that vary significantly among individuals and strongly influence drug-seeking behavior (Jhou et al., 2013; Ettenberg et al., 2015). In particular, animals exhibiting particularly strong conditioned place aversion (CPA) to cocaine are less prone to acquire operant drug-seeking behavior (Ettenberg et al., 1999, 2015; Jhou et al., 2013). To begin to elucidate these mechanisms underlying this phenomenon, we and others previously showed that conditioned avoidance to cocaine depends on the rostromedial tegmental nucleus (RMTg), a major GABAergic afferent to midbrain DA neurons, along with the lateral habenula (LHb), a major excitatory afferent to the RMTg (Lecca et al., 2011, 2012; Maroteaux and Mameli, 2012; Jhou et

Received July 14, 2020; revised Feb. 7, 2021; accepted Mar. 2, 2021.
Author contributions: J.P.-C., M.E., H.L., Y.S.C., and T.C.J. designed research; J.P.-C., M.E., H.L., and Y.S.C. performed research; J.P.-C., M.E., H.L., Y.S.C., and T.C.J. analyzed data; and J.P.C., M.E., and T.C.J. wrote the paper.
This work was supported by National Institute on Drug Abuse Grants T32-DA007288 (J.P.C.), R01-DA037327, U01-DA044468 (T.C.J.), and F30-DA048597 (Y.S.C.).
*J.P.-C. and M.E. contributed equally to this work.
The authors declare no competing financial interests.
Correspondence should be addressed to Thomas C. Jhou at jhou@musc.edu.
https://doi.org/10.1523/JNEUROSCI.1847-20.2021

al., 2013; Meye et al., 2015, 2016). However, although the neural mechanisms of cocaine avoidance are beginning to be elucidated, little is known about why these mechanisms vary so much among individuals. For example, cocaine induces activation of the immediate-early gene c-*fos* in the Entopeduncular nucleus (EPN), LHb, and RMTg after cocaine administration, but it is unknown whether these activations correlate with behavioral variation or whether they reflect underlying processes that might explain such variation. To address these questions, we used an operant runway self-administration model that is particularly sensitive to the negative motivational attributes of cocaine, in combination with *in vivo* recording, c-*fos*, pharmacological manipulations, and circuit-specific *in vitro* electrophysiological recordings. These methods demonstrated that cocaine-induced activation of the RMTg, but not upstream areas such as the LHb or EPN, correlate with individual differences in cocaine avoidance behavior. We further found that these differing levels of RMTg activation arise from a variety of cocaine-induced cellular alterations in ventral tegmental area (VTA)-projecting RMTg neurons, including calcium-permeable AMPA receptors (CP-AMPARs) but also presynaptic alterations.

Materials and Methods

Animals. All procedures were conducted under the National Institutes of Health Guide for the Care and Use of Laboratory Animals, and all protocols were approved by the Medical University of South Carolina Institutional Animal Care and Use Committee. Adult male Sprague Dawley rats weighing 200–300 × g from Charles River Laboratories were pair-housed in standard cages with food and water provided *ad libitum*, unless otherwise stated.

Intravenous catheterization and cocaine injections. Rats were anesthetized with isoflurane and fitted with indwelling intravenous catheters inserted into the right jugular vein, and subcutaneously passed to a guide cannula exiting the animal's back. After surgery, catheter patency was maintained via daily flushing with 0.05 ml of taurolidine-citrate solution. Animals recovered for 7 d before behavioral testing. Catheter patency was assessed periodically through observation of the loss of the righting reflex after intravenous injection of methohexital (Brevital, 2.0 mg/kg/0.1 ml). Rats that were unresponsive to Brevital were implanted with a new catheter into the left jugular vein.

In vivo *electrophysiological recordings.* Recordings were performed during once-daily sessions, 1–5 d after animals' last runway session, using methods similar to those we have previously published (Li et al., 2019a). In brief, baseline activity was recorded for 15 min, after which animals were given a single infusion of cocaine (0.75 mg/kg, i.v.). The recording apparatus consisted of a unity gain headstage (Neurosys) whose output was fed to preamplifiers with high-pass and low-pass filter cutoffs of 300 Hz and 6 kHz, respectively. Analog signals were converted to 18-bit values at a frequency of 15.625 kHz using a PCI digitizer card (National Instruments) and further analyzed by customized acquisition and analysis software (Neurosys). Preliminary spike detection was performed by thresholding to select waveforms at least 2 SDs above background noise levels, and waveforms were further classified using principal component analysis. Spikes were accepted only if they had a refractory period, determined by <0.2% of spikes occurring within 1 ms of a previous spike, as well as by the presence of a large central notch in the autocorrelogram. Neurons that had significant drifts in firing rates were excluded. Drivable electrode arrays were implanted above the RMTg (AP, −7.4 mm; ML, 2.1 mm; DV, −7.4 mm from dura, 10-degree angle). Electrodes were advanced 80–160 μm at the end of each session. Placements at RMTg were verified with FOXP1 stain (Smith et al., 2019).

c-fos *experiments.* Two to 5 d after the final runway trial, rats were given an i.p. injection of cocaine (10 mg/kg) followed 1 h later by transcardial perfusion with saline and 10% formalin. Brains were then removed and postfixed overnight in 10% formalin, equilibrated in 20% sucrose, sliced into 40 µm sections, and immunostained for c-*fos* as described previously (Smith et al., 2019). In brief, tissue was incubated overnight at room temperature in rabbit anti–c-*fos* [1:10K, Millipore, followed by incubation in secondary antibody (biotinylated donkey anti-rabbit, 1:1K, Jackson ImmunoResearch)], and visualization using avidin-biotin complex (Vector Laboratories) and diaminobenzidine.

Runway operant cocaine seeking. Methods are similar to our previous work (Jhou et al., 2013). Briefly, the runway consists of two opaque plastic compartments (start and goal, 25 × 10 × 17 cm length/width/height) connected by a 170-cm-long corridor with motorized sliding doors between the start/goal boxes and corridor. On test days, rats were tethered to an intravenous line, then placed into the start box for 30 s, after which doors were opened to allow free exploration of the apparatus. Entry into the goal box caused doors to close and a syringe pump to deliver cocaine [0.75 mg/kg, i.v., over 10 s, same dose as in conditioned place preference (CPP) and electrophysiological recording]. Rats then remained in the goal compartment for 5 min before being returned to the home cage. Failure to enter the goal compartment after 15 min resulted in a timeout. In such cases, animals were gently nudged by the experimenter into the goal box, given a cocaine infusion, and retained in the goal compartment for 5 min, ensuring that all animals received the same total exposure to both cocaine and the goal compartment. Before cocaine trials, animals received habituation trials in which animals freely explored the entire apparatus without cocaine. Rats received a minimum of two trials, which continued until two consecutive trials produced run latencies <60 s. Animals then received seven cocaine trials, at most twice daily and at least 4 h apart, ensuring that animals run in a cocaine-free state. All trials were run during the light period of the 24 h diurnal lighting cycle. In all trials, we tabulated both the latency to reach the goal box (after exiting the start box) as well as the number of run reversals, defined as a change in run direction spanning a minimum of two photobeams (~12 inches).

Progressive ratio and punishment resistance. Training procedures are identical to those we previously described (Vento et al., 2017). Briefly, animals are food restricted to 85% of initial body weight, trained to lever-press for food pellets (45 mg) until stable response rates were reached, then tested either on the progressive ratio (PR) task with progressively increasing effort requirements (lever-presses required per pellet) or progressively increasing punishment (i.e., a foot-shock of increasing intensity presented 1 s after food pellet delivery, whose magnitude increases ~25% every 3 trials). In the PR task, rats time out if 2 min passed without a lever press. In the punishment task, a timeout is defined by three consecutive trials with >30 s passing without a lever press. For both tasks, the break point is the last successfully completed ratio or shock intensity endured before timeout.

Novelty-induced locomotion. Novelty-induced locomotion was recorded in operant chambers placed inside sound-attenuating cabinets; movements within the chamber were detected via interruptions of an array of four photo-detector/emitter pairs. Locomotors counts were averaged over two sessions on consecutive days, which lasted for 30 min each.

CPP/CPA. We used an unbiased protocol in which the cocaine-paired side was chosen randomly for each rat, independently of preconditioning (baseline) bias. We used a three-chambered apparatus with two conditioning chambers (with dark- vs light-colored walls) and a small neutral center chamber. On day 1, animals were placed in the central chamber and allowed to explore all three chambers for 15 min, thus establishing a baseline preference score. On 4 subsequent days, rats received two conditioning sessions per day in which intravenous saline or cocaine (0.75 mg/kg) was infused in the morning or afternoon (counterbalanced within animals) in the home cage and then confined to one of the test chambers (either saline paired or cocaine paired) immediately (for CPP tests) or after remaining in the home cage for a 15 min delay (for CPA tests). One day after the final conditioning sessions, animals were given test sessions in which rats were placed into the central compartment and then allowed to freely explore all three compartments of the CPP apparatus for 15 min. Time spent in each compartment was recorded. The final preference score was calculated as the postconditioning preference (time in cocaine-paired chamber minus time in saline-

paired chamber) minus the preconditioning preference. Two separate tests (CPP and CPA) were conducted in each rat, in counterbalanced order, with three extinction sessions between the two tests in which rats explored all chambers without a drug. The preference score of the third extinction session was used as the new baseline for the second test.

Elevated plus maze. The elevated plus maze (EPM) consisted of two open (50 × 20 cm) and two enclosed arms (50 × 20 × 30 cm) and an open roof with the entire maze elevated 100 cm from the floor. Each rat was initially placed in the center of the EPM (facing toward open arm) to explore freely. Rats' behavior was recorded for 3 min by a video camera mounted centrally above the maze. The time spent in open versus closed arms of the maze was recorded and reported.

Intra-RMTg 1-naphthyl acetyl spermine administration. Cannula implantations in the RMTg were carried as described previously (Jhou et al., 2013). Briefly, under isoflurane (1.5–2%) rats were stereotaxically implanted bilaterally with 26 gauge guide cannulas (P1 Technologies) in the RMTg using the following coordinates: 7.2 mm posterior to bregma, 2.1 mm lateral to the sagittal suture, tips angled 10° toward the midline, 6.8 mm ventral to skull surface. Cannulas were held in place by dental acrylic, and patency was maintained with occlusion stylets. For intracranial injections, solutions were loaded bilaterally through 33-gauge injector cannulas, which extended 1.0 mm beyond the implanted guides. About 5 min after rats reached the goal box, 0.5 µl of 1-naphthyl acetyl spermine (NASPM; 80 µg/µl in saline; Tocris Bioscience) was infused into the RMTg of each hemisphere at 0.1 µL/min. Injector cannulas remained in place for another 60 s to allow drug diffusion, after which occlusion stylets were replaced and animals returned to their home cage. Equal volumes of saline were injected in control experiments. After completion of experiments, animals were killed and brains were extracted, snap frozen, and sliced into 40-μm-thick sections for cannula localization.

Brain slice preparation. Twenty to 24 h after the last runway trial, rats were anesthetized with isoflurane, decapitated, and their brain was quickly removed and placed in an ice-cold slicing solution containing (in mM): 92 N-Methyl-D-Glucamine (NMDG), 20 HEPES, 25 glucose, 30 $NaHCO_3$, 10 $MgCl_2$, 5.0 ascorbic acid, 3.0 sodium pyruvate, 2.5 KCl, 1.2 NaH_2PO_4, 0.5 $CaCl_2$, pH 7.4 (Ting et al., 2014). Coronal sections (~230 μm) containing the RMTg were obtained at a speed of 0.07 mm/s using a sapphire blade (Delaware Diamond Knives) in a vibrating microtome (Leica). Sections were subsequently incubated in the same cutting solution for 5 min at 32.0°C, before being transferred to artificial CSF (aCSF) containing the following (in mM): 126 NaCl, 2.5 KCl, 26 $NaHCO_3$, 2.5 $CaCl_2$, 1.5 $MgCl_2$, 1.25 NaH_2PO_4, and 10 glucose saturated with 95%/5% O_2/CO_2 for an additional 30 min at 32.0°C, followed by 30 min incubation at room temperature for at least 30 min before the recording commenced.

Ex vivo *electrophysiology.* RMTg slices were submerged in a recording chamber and superfused with ~32.5°C aCSF at a flow rate of 2 ml/min. Neurons were identified and visualized with a Nikon Eclipse E600FN microscope fitted with infrared differential interference contrast optics. In the RMTg all recordings were performed on cells expressing the fluorescent retrograde tracer cholera toxin B (CTB) subunit conjugated to Alexa Fluor 555 (300 nL, Invitrogen), which had been injected into the VTA [4.6 AP, 2.1, ML (10° angle), 7.8 DV] at least 14 d prior. Whole-cell electrophysiological recordings were obtained using borosilicate glass microelectrodes (tip resistance, 2.0–4.0 MΩ). In voltage clamp configuration recordings were performed using a patch pipettes backfilled with an internal solution containing (in mM): $CsMeSO_3H$ 130, NaCl 4, $MgCl_2$ 2, EGTA 0.3, HEPES 10, Mg_2ATP 2, Na_3GTP 0.2, QX-314 3, pH ~7.3, and 280–285 mOsm, whereas current-clamp recordings were performed with a pipettes backfilled with (in mM): K-gluconate 140, NaCl 5, HEPES 20, EGTA 0.2, MgCl2 2, Mg_2ATP 4, Na_3GTP 0.2, pH ~7.3, and 280–285 mOsm. For the biocytin filling, 2 mg/ml biocytin was added in the internal solution. Access resistance was monitored with a 20 ms step of −5 mV and maintained below 20 MΩ, and recordings were accepted for analysis if changes in access resistance were <15% over the recording duration. Electrophysiological signals were amplified using the Multiclamp 700A amplifier (Molecular Devices), low-pass filtered at 2 kHz, and digitized at 10 kHz. Data were collected using AxoGraph X and stored for offline analysis.

To evoke postsynaptic currents, excitatory afferents were stimulated (100–200 µs duration) with a bipolar tungsten electrode (FHC) positioned immediately dorsal or dorsomedial (within 50–100 μm) to the recorded cell. For EPSC paired-pulse ratio (PPR), the cell was held at −70 mV, and two stimuli (200 µs duration each, 50 ms apart, amplitude adjusted to achieve ~40–50% of maximum amplitude) were applied every 20 s in the presence of picrotoxin 100 μM. The PPR was then calculated by dividing the amplitude of the second evoked EPSC by the first. To measure the AMPA/NMDA ratio, cells were held at –70 mV for 5 to 10 min to ensure stability and then were depolarized to +40 mV. Raw EPSC currents were then monitored for 5 to 10 min at +40 mV, and AMPA currents were isolated by applying the NMDA receptor antagonist D-AP5 (50 μM). The NMDA current component was obtained by subtracting the isolated AMPA current from the total current. The AMPA/NMDA ratio was calculated by dividing the peaks of the AMPA over the NMDA. Spontaneous EPSCs (sEPSCs) were recorded at −70 mV in presence of picrotoxin 100 μM for 5–10 min. sEPSCs were detected by Axograph using a sliding template algorithm with a threshold at three times the background noise SD (typically ~7 pA), and decay, amplitude, and frequency were calculated from the average of all events for each neuron. To measure the AMPAR rectification index, D-AP5 (50 μM) was included in the aCSF to block NMDAR currents, and spermine (100 μM) was added to the internal solution. AMPAR EPSCs were evoked from −70 to +40 mV in 10 mV step at 0.05 Hz, and the rectification index calculated using the equation rectification index (R.I.) = EPSC amplitude at −70 mV/EPSC amplitude at +40 mV. To pharmacologically confirm the presence of calcium-permeable AMPA receptors, the (CP-AMPAR) blocker NASPM (100 μM) was bath applied for 10 min in the presence of picrotoxin (100 μM) and D-AP5 (50 μM). AMPAR rectification indexes were also measured by photolytic uncaging of the caged glutamate MNI-glutamate (100 μM). In these experiments, we added TTX (1 μM), MK-801 (20 μM), picrotoxin (100 μM), MTEP (5 μM), and JNJ-16259685 (5 μM) to the aCSF to block Na_V, NMDAR, GABA-A, and mGluR1/5 currents, and this bath solution was recirculated for at least 10 min before recording. The experiments were conducted in the dark, and uncaging of MNI-glutamate was conducted with 5–15-ms UV light pulses of wide-field illumination (365 nm LED, Thorlabs; coupled through a 40× objective (Nikon, numerical aperture 0.8). Light power and duration were controlled via the LED driver (LEDD1B, Thorlabs) by external voltage modulation. AMPAR excitatory postsynaptic currents were evoked at −70 mV, 0 mV, and +40 mV every 60 s, and the rectification index was calculated using the equation R.I. = EPSC amplitude at −70 mV/EPSC amplitude at +40 mV. Cell excitability was assessed in current clamp using input-output (I-O) curves of incremental current injections steps, during which we tabulated the number of spikes during each current step. The input resistance was derived using the slope from the steady-state during the hyperpolarization step.

Statistical analysis. Analysis between two groups was made using two-tailed Student's *t* test (unpaired *t* test for comparison between two groups, paired *t* test for comparison within the same group). One- or two-way ANOVA was used as appropriate, followed by Tukey's *post hoc* tests. Statistical results are presented as mean ± SEM. All statistical analysis was performed using GraphPad Prism (version 7.0), and results were considered significant for $p < 0.05$.

Results

Individual rats display large variations in cocaine avoidance

In previous work, we and others characterized aversive responses to cocaine using CPP and a runway operant task developed over two decades by Ettenberg et al. (1999), and more recently adopted by our lab (Jhou et al., 2013; Li et al., 2020). However, those studies did not have sufficiently large group sizes to fully characterize the distribution of individual variations in cocaine aversion. Hence, we tested 105 Sprague Dawley rats on runway operant cocaine seeking, in which animals were placed at one end of a 5-foot-long corridor and allowed to run to the opposite

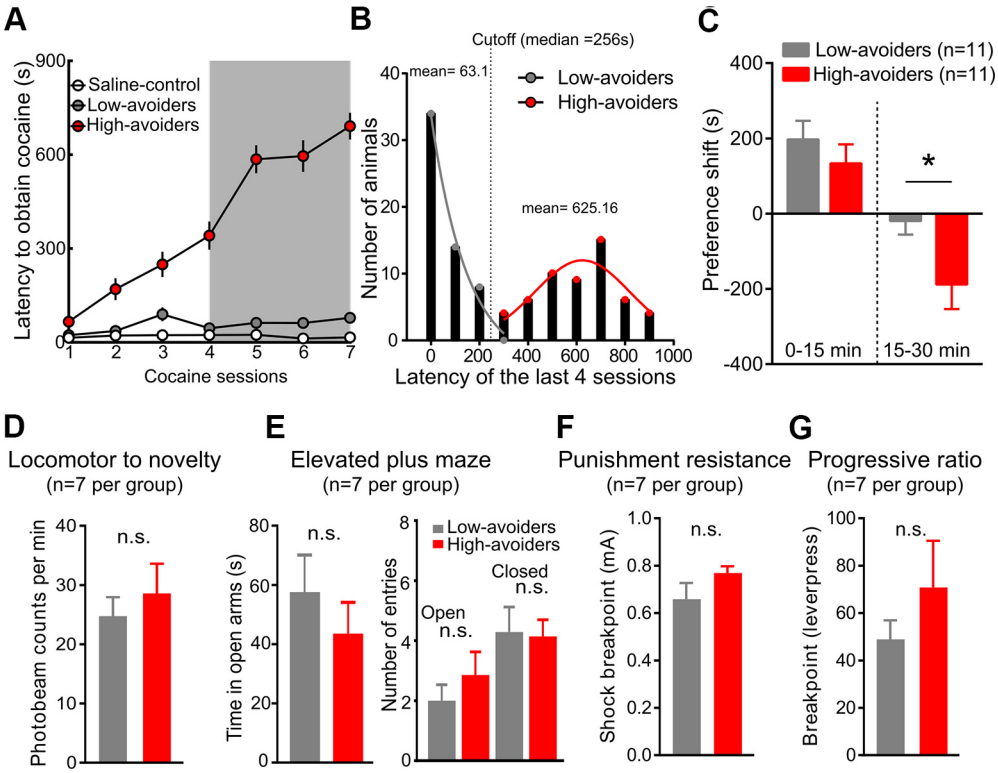

Figure 1. Individual rats show large variations in cocaine avoidance. ***A***, In a runway operant cocaine-seeking task, roughly half of all animals gradually developed avoidance latencies to cocaine > 256 s (high-avoiders), whereas the others did not (low-avoiders). ***B***, A histogram of the average run latency of the last four cocaine sessions shows a bimodal distribution, identifying separate high- and low-cocaine avoider populations. ***C***, High- and low-avoider rats developed similar levels of place preference to rewarding effects of cocaine 0–15 min postinfusion, whereas high-avoiders showed greater place aversion to cocaine than low-avoiders 15–30 min postinfusion. ***D–G***, High- and low-avoiders were not different in at least four nondrug tasks: novelty-induced locomotion, elevated plus maze, punishment resistance, and progressive ratio. Error bars indicate mean ± SEM, ∗ indicates $p < 0.05$.

end to receive a single dose (0.75 mg/kg, i.v.) of cocaine delivered intravenously on entry into the goal box. Consistent with previous work, these rats showed on average a gradual increase in latencies over seven trials but with average latencies also varying considerably between individuals over the last four sessions (Fig. 1*A*). Interestingly, average latencies per animal were bimodally distributed (Fig. 1*B*), with two roughly equal size peaks separated by a median of 256 s residing in the valley between peaks. Hence, we subsequently grouped animals into high or low avoiders using this threshold.

In principle, higher latencies to obtain cocaine in the runway task can reflect either higher aversive effects of cocaine or lower rewarding effects. To distinguish these possibilities, we tested each animal twice on a CPP task, once with animals confined to conditioning chambers 0–15 min after receiving cocaine, and a second time (in counterbalanced order) with animals confined to conditioning chambers 15–30 min after receiving cocaine (Fig. 1*C*). Prior reports using this paradigm found that cocaine induces a place preference in the first condition but a place aversion in the second (Ettenberg et al., 1999; Knackstedt et al., 2002). Analysis of the current experiment using a repeated measures two-way ANOVA confirmed that the two delay conditions produced different preference scores ($F_{(1,20)} = 17.43$, $p = 0.0005$), and further showed a difference between low- and high-avoider groups ($F_{(1,20)} = 7.318$, $p = 0.0136$), with no significant interaction ($F_{(1,20)} = 1.829$, $p = 0.1913$). *Post hoc* testing further showed that high and low avoiders showed similarly high levels of cocaine preference in the 0–15 min condition (Fig. 1*C*; Tukey's test, $p = 0.8293$), whereas in the 15–30 min condition, high avoiders showed stronger place aversion than the low avoiders (Tukey's test, $p = 0.035$). Hence, variation in cocaine avoidance in the runway task was associated with differences in cocaine's delayed aversive effects but not its immediate rewarding effects.

We next examined whether aversive responses to cocaine could have been confounded by other behavioral variables, such as novelty-induced locomotion or anxiety, which could affect run latencies independently of the response to cocaine. We found that low and high avoiders showed similar locomotor responses to a novel chamber (unpaired *t* test, $t_{(9)} = 0.61$, $p = 0.55$) when tested 24 h after the last runway trial, and similar levels of anxiety-like behavior in the EPM (unpaired *t* test, $n = 7$ per group; open arm time, $t_{(12)} = 0.01{,}617$, $p = 0.9874$; closed arm time, $t_{(12)} = 0.3053$, $p = 0.7654$; open arm entries, $t_{(12)} = 0.9150$, $p = 0.3782$; closed arm entries $t_{(12)} = 0.1424$, $p = 0.8891$, Fig. 1*D*, *E*). Low and high avoiders also did not differ in a progressive ratio food-seeking task (unpaired *t* test, $t_{(9)} = 0.95$, $p = 0.37$), nor a progressive punishment food-seeking task we previously used to measure the ability of a foot-shock punisher to inhibit food-seeking (unpaired *t* test, $t_{(10)} = 1.5$, $p = 0.17$, Fig. 1*F–H*; Li et al., 2019b), further suggesting that drug-seeking behavior on the runway is not secondary to generalized differences in nondrug motivation, nor does it reflect general deficits in aversive learning.

High cocaine avoiders show greater neuronal activation in the RMTg but not upstream sites

Having observed that runway cocaine avoidance differs greatly among animals, and correlates with differing place aversion responses to cocaine, we next sought to identify the neural substrates of these individual differences. Previous work has

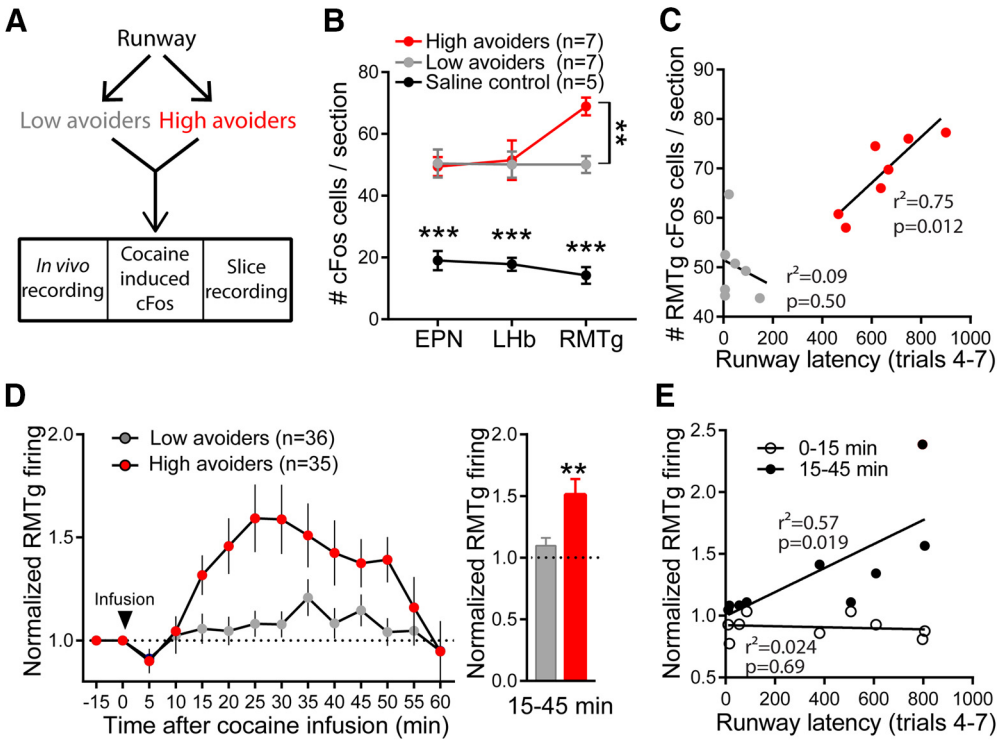

Figure 2. High- and low-cocaine avoiders show distinct responses to cocaine in EPN, LHb, and RMTg. ***A***, Schematic of experimental design, in which animals are screened on operant runway cocaine seeking, categorized into high and low-avoiders, and then subjected to recording and/or c-*fos* measurements. ***B***, Cocaine increased c-*fos* in rEPN, LHb, and RMTg (red/gray symbols), relative to saline, which produced only minimal c-*fos* (black symbols), but only the RMTg showed greater cocaine-induced c-*fos* in high versus low-avoiders. ***C***, RMTg c-*fos* positively correlated with runway latency within the high-avoider but not the low-avoider group. ***D***, *In vivo* recordings of RMTg neurons in awake behaving rats showed robust activation in high but not low-avoiders 15–45 min after cocaine infusion. ***E***, Average RMTg responses in individual rats 15–45 min but not 0–15 min after cocaine infusion positively correlated with runway latency. Error bars indicate mean ± SEM, ∗ indicates $p < 0.05$, ∗∗ indicates $p < 0.01$, ∗∗∗ indicates $p < 0.001$.

identified the serially connected EPN, LHb and RMTg brain regions as key drivers of aversive reactions to cocaine (Jhou et al., 2013; Meye et al., 2015, 2016). However, it is not known whether individual differences in behavior are because of variations in function of one or more of these regions. Hence, in a subset of rats screened for cocaine avoidance, we examined cocaine-induced expression of the immediate early gene c-*fos* in the EPN, LHb, and RMTg. After a single infusion of cocaine given 1 h before being killed, c-*fos* counts in the RMTg, EPN, and LHb, were all higher than in rats receiving saline (one-way ANOVA, Tukey's test, $n = 5$–7 per group; RMTg, $F = 86.9$, $p = 0.0001$; LHb, $F = 12.53$, $p = 0.0013$ low avoiders vs saline, $p = 0.0009$ high avoiders vs saline; EPN, $F = 19.5$, $p = 0.0001$; Fig. 2*B*). Furthermore, cocaine-induced c-*fos* in the RMTg (but not EPN and LHb) was much higher in high- than low-avoider rats [Fig. 2*B*; two-way ANOVA $n = 5$–7 per group, $F_{(2,16)} = 64.7$, $p = < 0.0001$, effect of group (high vs low vs saline), $F_{(4,32)} = 3.4$, $p = 0.020$, interaction of region x group, Tukey's test, $p = 0.025$, RMTg high vs low avoider, $p > 0.99$ for rEPN and LHb high vs low avoider]. We further found that c-*fos* in the RMTg not only correlated with the variations between high- and low-avoider groups but also correlated with variations observed within the high-avoider group, as c-*fos* cells in the RMTg positively correlated with the mean latency of the last four sessions within the high avoider group but not the low avoider group ($r^2 = 0.75$, $p = 0.012$; $r^2 = 0.092$, $p = 0.51$, respectively; Fig. 2*C*).

Because c-*fos* is an indirect measure of neuronal firing with poor temporal resolution, we further evaluated RMTg electrophysiological responses to cocaine in awake rats in 35 neurons from 11 high avoiders and 36 neurons from 13 low avoiders (Fig. 2*D*). RMTg neurons in both groups showed decreased firing during the first 15 min after cocaine infusion (when cocaine is rewarding), that did not differ between high and low avoiders ($t_{(57)} = 0.097$, $p = 0.92$). However, high avoiders showed significantly higher firing relative to low avoiders 15–45 min after cocaine infusion, overlapping the period when cocaine is aversive (unpaired *t* test, $n = 26$–32 per group, $t_{(56)} = 3.97$, $p = 0.0034$; Fig. 2*D*). Correlation analysis in individual rats revealed that RMTg neuron responses 15–45 min but not 0–15 min postcocaine infusion positively correlated with individual's runway latency (Fig. 2*E*; $r^2 = 0.57$, $p = 0.015$ and $r^2 = 0.02$, $p = 0.69$).

Cocaine-avoiding rats exhibit enhanced excitability of VTA-projecting RMTg neurons

The above results indicate that cocaine avoidance correlated with activation of the RMTg (measured using both c-*fos* and firing) but not with c-*fos* in upstream regions such as the LHb or EPN. This result seems at odds with our previous findings that cocaine avoidance critically depends on LHb and EPN activation (Jhou et al., 2013; Li et al., 2020). To resolve this apparent contradiction, we hypothesized that cocaine avoidance driven by the RMTg might indeed depend on excitatory inputs but that the RMTg may be more responsive to excitatory inputs in high avoiders than low avoiders. Hence, we measured intrinsic neuronal excitability in VTA-projecting RMTg neurons, by injecting the retrograde tracer CTB-555 into the VTA and measuring excitability of RMTg neurons using whole-cell current clamp electrophysiology. Interestingly, depolarizing current injections elicited a greater number of action potentials in neurons obtained from high-avoider rats than saline-control and low-avoider rats at injected currents ranging from 20 to 160 pA (two-way ANOVA repeated-measures

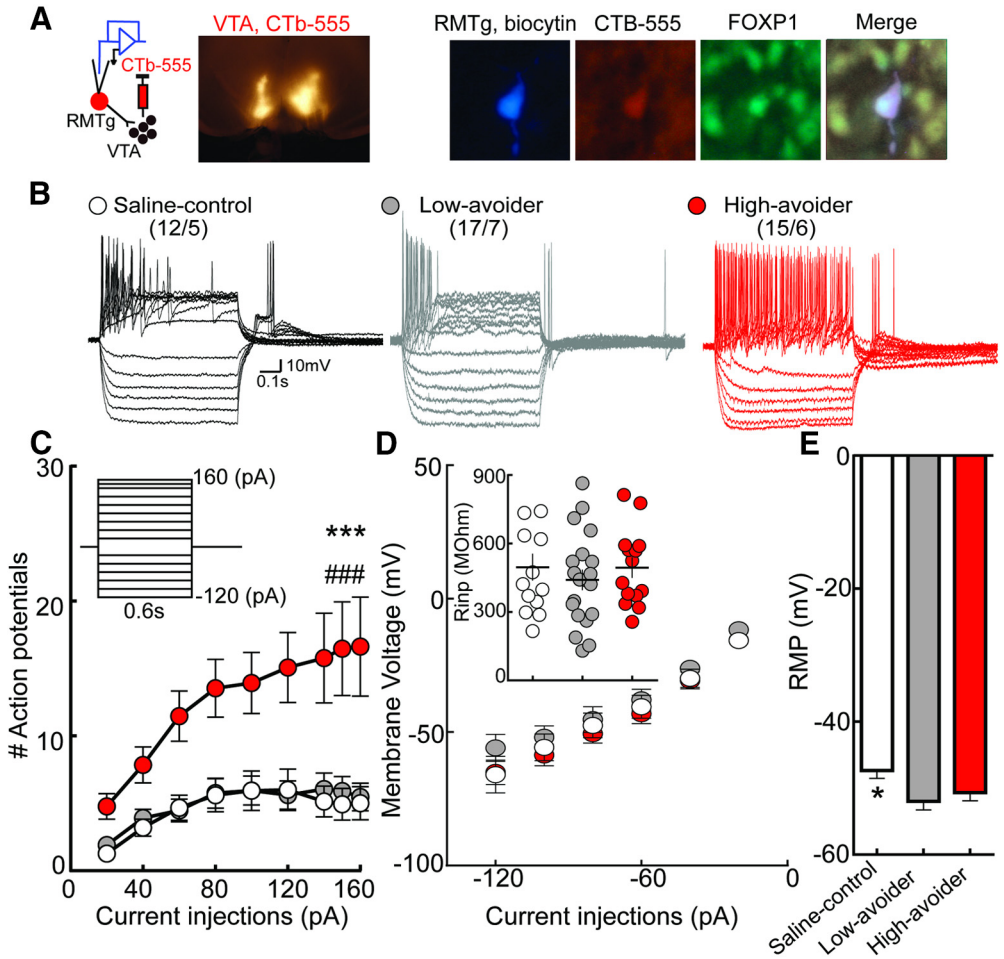

Figure 3. Cocaine increases excitability in VTA-projecting RMTg neurons from high- but not low-avoider rats. ***A***, Top left, photomicrographs showing injection of CTB-555 in the VTA. Top right, High-magnification immunofluorescent images showing triple label of biocytin, CTB-555, and the RMTg marker FoxP1. ***B***, Representative voltage traces in response to current injection (−120 to +160 pA) in high and low-avoiders, and controls running to receive saline instead of cocaine. ***C***, I–O curve collected from current (20–160 pA) injected into VTA-projecting RMTg neurons from saline-control, low-avoider, and high-avoider rats. Cells from high-avoiders showed elevated average firing, compared with saline control and low-avoiders. ***D***, Input resistance of VTA-projecting RMTg neurons did not differ between cocaine avoidance phenotypes. ***E***, VTA-projecting RMTg neurons from low-avoiders displayed a more hyperpolarized membrane potential than saline control but was not different from high-avoiders. Cells/rats per group are denoted in the corresponding graph. Error bars indicate mean ± SEM, ∗ indicates $p < 0.05$, ∗∗∗ indicates $p < 0.0001$ high-avoiders versus low-avoiders, ### indicates $p < 0.0001$ saline control versus high-avoiders.

ANOVA, interaction, $F_{(16,368)} = 2.32$, $p = 0.0029$; phenotypes, $F_{(2,46)} = 10.36$, $p = 0.00{,}019$; injected current, $F_{(2,368)} = 17.35$, $p = 1.0 \times 10^{-6}$; Fig. 3*B*,*C*). These differences were largely because of saline- and low-avoider rats showing a rapid accommodation to current-evoked firing that was attenuated or lost in high-avoider rats, leading to a significant upward shift in the current-spike response curves obtained from high avoiders, indicating a facilitation in evoked firing (Tukey's *post hoc* test, high-avoiders vs saline-control, 160 pA current step, $p = 0.0001$; high avoiders vs low avoiders, 160 pA current step, $p < 0.0001$; saline-control vs low avoider 160 pA current step, $p = 0.97$; Fig. 3*C*). These differences were not because of changes in passive membrane properties such as input resistance (R_{inp}), which were similar in all groups (one-way ANOVA, $F_{(2,44)} = 0.45$, $p = 0.6401$; R_{inp}: 496.2 ± 58.7, 440.7 ± 44.9, and 494.4 ± 44.9 MΩ for cocaine-naive, low and high avoiders respectively; Fig. 3*D*). We did see an alteration in the resting membrane potential (RMP) in low-avoider rats, as it was significantly more hyperpolarized than cocaine-naive rats (One-way ANOVA, $F(2, 45) = 3.6$, $p = 0.034$) saline-control versus low-avoiders (Tukey's test: $p = 0.027$), but was not different from the high-avoider group. However, this alone does not explain the differences in depolarization-evoked responses as the saline and low-avoider groups showed similar depolarization-evoked firing despite the different RMPs, whereas the low- and high-avoider groups showed different evoked firing despite having similar RMPs.

In addition to intrinsic excitability, we next sought to also characterize excitatory synaptic transmission onto the RMTg in high- and low-cocaine avoider rats. We found that high- and low-avoider rats showed a significant difference in sEPSC frequency (Fig. 4*B*; one-way ANOVA, $F_{(2,45)} = 10.4$, $p = 0.0017$) but not amplitude (Fig. 4*C*; one-way ANOVA, $F_{(2,45)} = 2.24$, $p = 0.09$). In particular, high-avoider rats had a higher sEPSC frequency compared with both saline controls (Fig. 4*B*; Tukey's test, $t = 3.859$, $p = 0.024$) and low avoiders (Fig. 4*B*; Tukey's test, $p = 0.00{,}011$), but no difference were seen between saline controls and low avoiders (Fig. 4*B*; Tukey's test, $p = 0.82$), consistent with presynaptic alterations. To further assess presynaptic differences, we used the PPR and found a significantly decreased PPR (Fig. 4*D*; one-way ANOVA, $F_{(2,46)} = 7.6$, $p = 0.0014$) in the high avoiders compared with both low avoiders (Tukey's test, $p = 0.0017$) and saline controls (Tukey's test, $p = 0.021$) but not

between saline control and low avoider (Tukey's test, $p = 0.87$), consistent with increased glutamate release probability in high avoiders. In addition to these presynaptic effects, analysis of sEPSC decay times revealed faster decay times (Fig. 4*E*; one-way ANOVA, $F_{(2,45)} = 6.6$, $p = 0.003$) in low-avoider rats compared with saline (Tukey's test, $p = 0.02$) and versus high-avoider rats (Tukey's test, $p = 0.004$) but not between saline control and high avoider (Tukey's test, $p = 0.84$), consistent with altered postsynaptic function.

Although spontaneous EPSC amplitudes (presumably reflecting postsynaptic function) were not different among groups, our observation of slower sEPSC decay times in high avoiders suggests possible postsynaptic differences that had not been detected in the sEPSC measures. In particular, prior studies had found that slow decay kinetics in AMPARs containing subunits that conferred greater calcium permeability, inward rectification, and sensitivity to NASPM (Bowie and Mayer, 1995; Bowie et al., 1998; Isaac et al., 2007; Stincic and Frerking, 2015; Erlenhardt et al., 2016; Wang et al., 2017). Hence, we calculated the R.I. from *I–V* curves constructed from pharmacologically isolated AMPAR-mediated eEPSCs in VTA-projecting RMTg neurons in the presence of intracellular spermine (100 μM; Fig. 5*A*). Indeed, we detected strong inward rectification in saline control and high-avoider rats (R.I.: saline control = 0.45 ± 0.047; high avoiders = 0.42 ± 0.046; Fig. 5*A*, inset), supporting the presence of synaptic CP-AMPARs in these groups. In contrast, low avoiders displayed more linear *I–V* relationships in the AMPAR-eEPSC than the other two groups (R.I.: 0.81 ± 0.12; Fig. 5*A*, inset; one-way ANOVA, $F_{(2,23} = 6.1$, $p = 0.0077$, Tukey's test, $p = 0.029$ low avoider vs saline, $p = 0.0071$ low avoider vs high avoider, $p = 0.90$ saline vs high avoider), consistent with lower proportions of CP-AMPARs (Isaac et al., 2007; Clem and Huganir, 2010). We further examined AMPAR subunit composition in VTA-projecting RMTg neurons using NASPM (100 μM), a selective pharmacological blocker of CP-AMPAR-mediated EPSCs (100 μM; Fig. 5*B*). We found that NASPM reduced AMPA EPSC amplitudes in saline control and high-avoider rats but not low avoider rats (two-way repeated measures ANOVA: phenotypes, $F_{(2,22)} = 4.1$, $p = 0.032$; time, $F_{(15,330)} = 7.1$, $p = 0.0001$; interaction, $F_{(30,330)} = 3.05$, $p = 0.0001$, Tukey's test, $p = 0.036$ low avoider vs saline, $p = 0.049$ low avoider vs high avoider, $p = 0.98$ saline versus high avoider). These results are all consistent with higher CP-AMPARs in RMTg in the saline and high-avoider groups compared with low avoiders. However, those experiments used electrically evoked eEPSCs, whose amplitudes could be confounded by known effects on presynaptic release of the many postsynaptic depolarization steps used in our R.I. tests (Kreitzer and Regehr, 2001; Wilson and Nicoll, 2001; Ohno-Shosaku et al., 2002; Kreitzer and Malenka, 2005; Crepel and Daniel, 2007; Crépel et al., 2011). Hence, to control for possible presynaptic differences in electrically evoked glutamate, we repeated the R.I. tests using photolytically uncaged glutamate while blocking presynaptic transmission with TTX. We also added MK-801, picrotoxin, MTEP, and JNJ-16259685 to block NMDA, GABA-A, and mGluR1-5 receptors, respectively (the latter being extrasynaptic, and hence particularly prone to activation by uncaged glutamate versus electrical stimulation). Consistent with R.I. measured using electrically evoked eEPSCs, the R.I. ratio calculated using uncaged

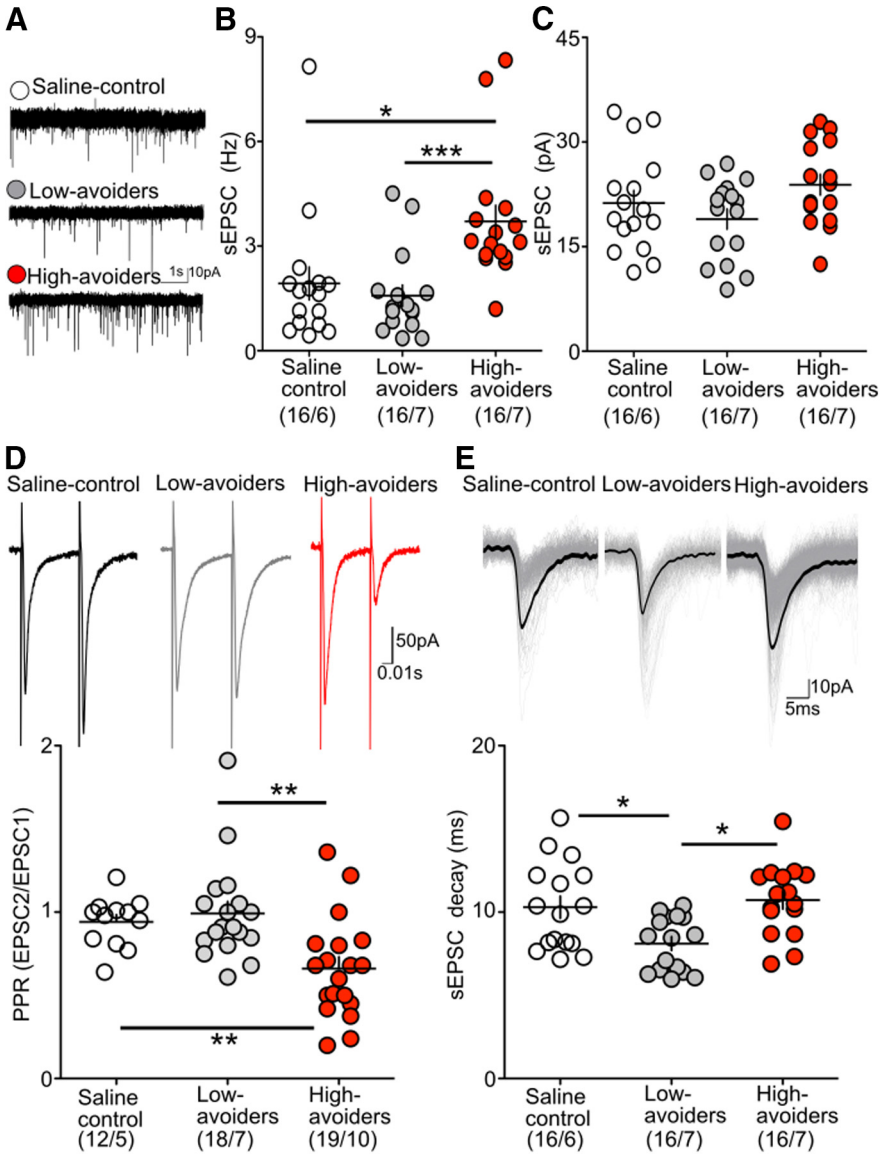

Figure 4. Cocaine increases excitatory presynaptic transmission onto VTA-projecting RMTg neurons of high- but not low-avoider rats. ***A***, Representative raw traces of sEPSCs in VTA-projecting RMTg neurons from saline-control, low-avoider, and high-avoider rats. ***B***, VTA-projecting RMTg neurons from high-avoiders showed elevated sEPSC frequency, compared with saline control and low-avoiders. ***C***, sEPSC amplitudes of VTA-projecting RMTg neurons were not affected by cocaine or avoidance phenotypes. ***D***, Top, representative eEPSC traces evoked by paired pulses 50 ms apart. Bottom, VTA-projecting RMTg neurons from high-avoiders displayed lower PPR than saline control and low-avoiders. ***E***, Top, sEPSC traces from one representative cell in each condition used for decay time assessment. Average is shown with thicker black trace. Bottom, VTA-projecting RMTg neurons from low-avoiders displayed lower sEPSC decay time (s) than saline control and high-avoiders. Cells/rats per group are denoted in the corresponding graph. Error bars indicate mean ± SEM, * indicates $p < 0.05$, ** indicates $p < 0.01$, *** indicates $p < 0.0001$.

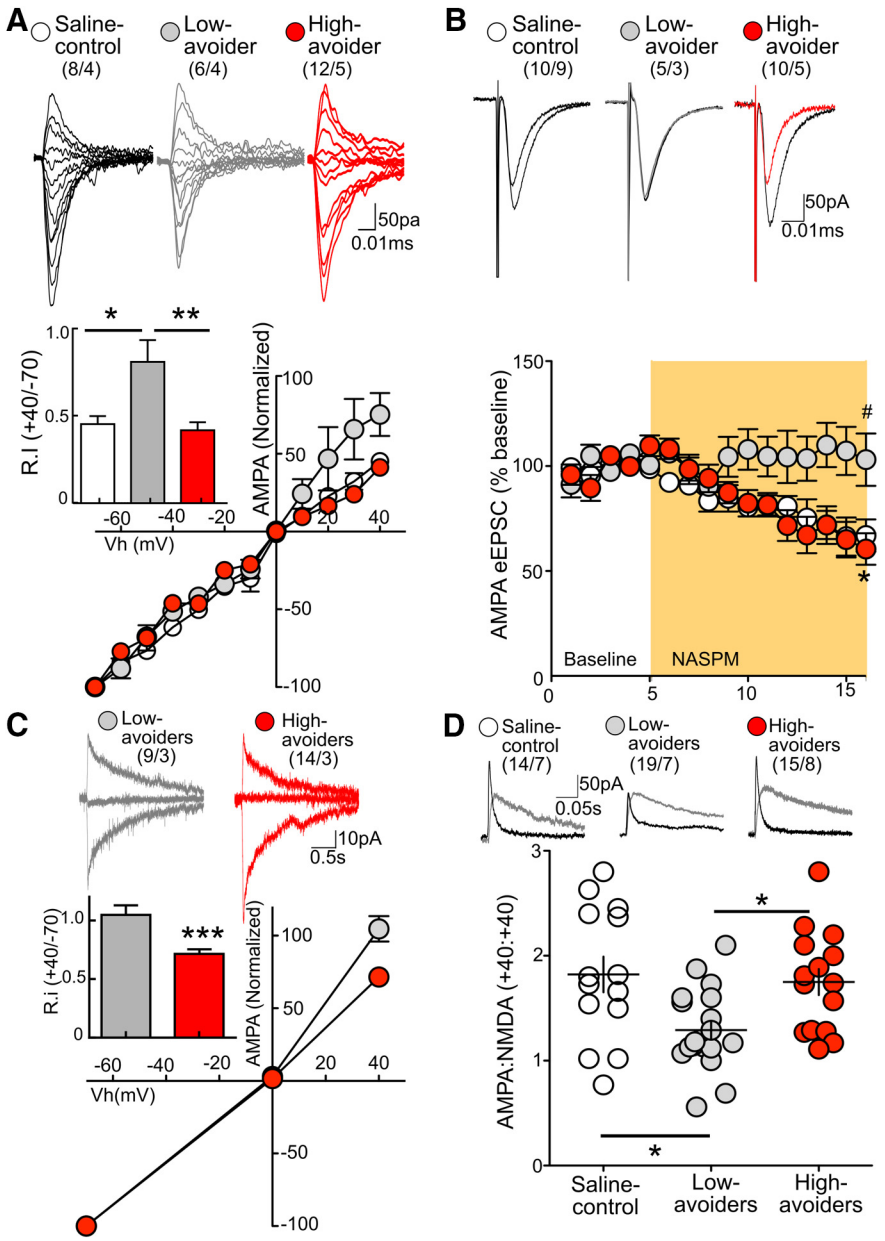

Figure 5. Cocaine decreases excitatory postsynaptic transmission onto VTA-projecting RMTg neurons of low- but not high-avoider rats by alterations in CP-AMPA receptors. ***A***, Top, representative traces of AMPAR EPSCs recorded at holding potentials from −70 to +40 in 10 mV steps in VTA-projecting RMTg neurons from saline-control, low-avoider, and high-avoiders rats. Bottom, *I–V* plots of normalized AMPAR eEPSC from the same groups. Inset, VTA-projecting RMTg neurons from saline control and high-avoiders displayed greater inward rectification (lower ratio of eEPSC at +40 to −70mV holding) than low avoiders. ***B***, Top, representative eEPSC traces recorded at −70 mV before and after administration of the CP-AMPA blocker NASPM (100 μM) in VTA-projecting RMTg neurons from saline-control, low-avoider, and high-avoider rats. Bottom, NASPM decreased evoked eEPSC in both saline-control and high-avoider but not low-avoider rats. ***C***, Top, representative traces of AMPAR EPSCs evoked by uncaged glutamate at −70, 0, and +40 mV holding, in VTA-projecting RMTg neurons from low- and high-avoider rats. Bottom, *I–V* plots of normalized AMPAR eEPSC from low- and high-avoider rats. Inset, VTA-projecting RMTg neurons from high-avoiders displayed greater inward rectification than low-avoiders. ***D***, Top, representative traces illustrating AMPA and NMDA eEPSC recorded at +40 mV in VTA-projecting RMTg neurons. Bottom, low-avoiders displayed lower AMPA:NMDA ratios than saline-control and high-avoiders. Cells/rats per group are denoted in the corresponding graph. Error bars indicate mean ± SEM, * indicates $p < 0.05$, ** indicates $p < 0.01$, *** indicates $p < 0.001$ high-avoiders versus low-avoiders, and # indicates $p < 0.05$ saline-control versus low-avoiders.

glutamate showed a stronger inward rectification in high avoiders than low avoiders (R.I.: high avoiders = 0.60 ± 0.046; low avoiders 0.95 ± 0.12; unpaired *t* test $t_{(21)} = 3.7$, $p = 0.0013$; Fig. 5*C*, inset), again consistent with a higher proportion of CP-AMPARs. EPSCs were mediated by AMPARs as they were blocked by NBQX (data not shown). Interestingly, in comparison to electrically evoked AMPA-EPSCs, AMPA-EPSCs evoked by photolytic glutamate uncaging had slower decay times, possibly because of the additional activation of extrasynaptic AMPA receptors by uncaged versus synaptically stimulated glutamate. Our evidence for greater CP-AMPARs, combined with the higher single-channel conductance of these receptors relative to calcium-impermeable AMPA receptors CI-AMPARs (Verdoorn et al., 1991; Jonas and Burnashev, 1995; Swanson et al., 1997; Liu and Zukin, 2007) led us to hypothesize that VTA-projecting RMTg neurons in high-avoider rats (and saline controls) would show higher AMPA/NMDA ratios than low avoiders, reflecting stronger excitatory transmission (Malinow and Malenka, 2002). Indeed, compared with low-avoider rats, saline-control and high-avoider rats had significantly higher AMPA/NMDA ratios (one-way ANOVA, $F_{(2,45)} = 5.71$, $p = 0.0061$; Tukey's test, saline vs low avoiders, $p = 0.011$; low vs high avoiders, $p = 0.025$; saline versus high avoiders, $t = 0.39$, $p = 0.999$).

Our findings of large synaptic differences between low and high avoiders after cocaine exposure raises the question of whether these differences are present beforehand or arise in response to cocaine exposure. If present beforehand, one would expect a bimodal distribution of glutamatergic synaptic properties in saline control rats, reflecting the as yet undetermined cocaine avoidance phenotypes. However, to our surprise, we found that saline control rats uniformly expressed high AMPA/NMDA ratios, reflecting postsynaptic potentiation similar to that seen in high avoiders (high AMPA/NMDA; Fig. 6*A*). Furthermore, saline rats also expressed high PPRs, reflecting presynaptic depotentiation similar to low avoiders (high PPR; Fig. 6*A*). Hence, cocaine-naive rats exhibit a mismatch between pre- versus postsynaptic states not present in either low or high avoiders.

The above findings suggest that cocaine exposure drives multiple types of plastic changes in the RMTg, one of which is a decrease in RMTg CP-AMPAR responses selectively in low-avoider rats. To determine whether this reduction in CP-AMPARs could contribute to reduced behavioral cocaine avoidance in these rats, we tested whether blocking CP-AMPARs with NASPM would reduce aversion to cocaine. Indeed, in 10 rats that received intra-RMTg infusion of NASPM, we observed a faster latency to reach the goal box than 9 rats receiving saline (unpaired *t* test, $t_{(17)} = 3.075$, $p = 0.0069$; Fig. 6*D*).

From four additional rats in which NASPM was infused outside the RMTg because of cannula misplacement, we found that two rats were high avoiders (latencies 429 and 900 s), and two were low avoiders (latencies <30 s), a similar proportion as observed in untreated rats, suggesting that the CP-AMPAR influence on cocaine avoidance has some anatomic selectivity for the RMTg. Together, these data suggest that variation in CP-AMPARs in the RMTg could drive variability in cocaine aversion and, in turn, the motivation to seek cocaine.

Discussion

In the present study, we found evidence that cocaine's aversive effects, as measured using both a runway operant task and CPP/CPA tests, show large variations among rats that depend on specific alterations in function of the RMTg, a structure we and others previously showed drives avoidance responses to cocaine and other stimuli (Stamatakis and Stuber, 2012; Jhou et al., 2013; Sánchez-Catalán et al., 2016; Proulx et al., 2018; Smith et al., 2019; Li et al., 2019b, 2020). In particular, we found that individual SD rats are roughly equally divided between high versus low avoiders of cocaine, and that these two groups differed markedly in cocaine-induced RMTg activation. We further identified several possible cellular mechanisms of this difference, as high avoiders showed greater RMTg firing in response to depolarizing current steps, along with greater pre- and postsynaptic responses to glutamatergic stimulation. Interestingly, differential responses to cocaine (as measured by c-*fos*) were not seen in structures upstream from the RMTg (LHb and EPN), although they are also activated by cocaine and also drive avoidance responses to cocaine (Jhou et al., 2013; Gao et al., 2018). Hence, the current study suggests that differential RMTg responses to cocaine may be because of its differential sensitivity to excitatory cocaine-activated inputs rather than differential activity in these input structures per se.

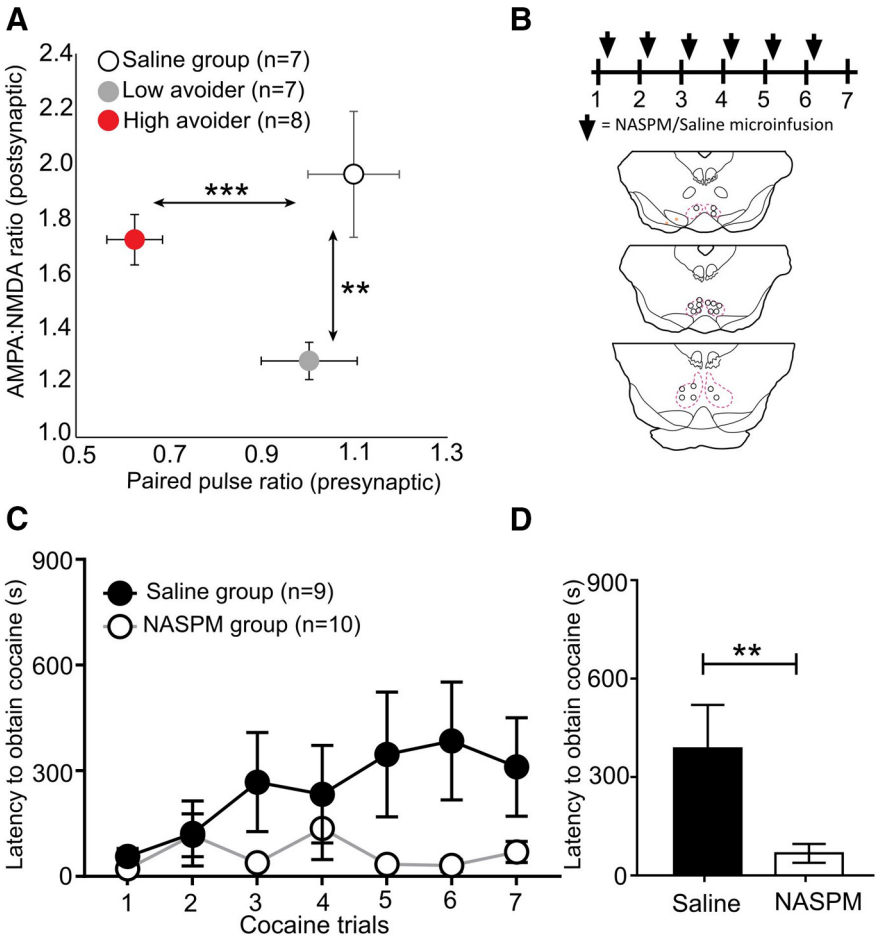

Figure 6. CP-AMPARs in RMTg contribute to cocaine avoidance behavior. ***A***, Relationships between postsynaptic strength (AMPA:NMDA ratio) and presynaptic strength (PPRs) in VTA-projecting RMTg neurons. Saline-control rats displayed high AMPA/NMDA ratios and PPRs. Cocaine exposure selectively decreased PPRs in high but not low avoiders, and AMPA/NMDA ratios in low but not high avoiders. ***B***, Top, schematic timeline course for experimental behavioral paradigm shows NASPM or vehicle infusion after each runway trial. Bottom, location of infusion sites of the CP-AMPAR receptor antagonist NASPM (open symbols) or vehicle (black-filled symbols), delivered into the RMTg 10 min after rats reached the runway goal box in each trial. ***C***, NASPM significantly reduced runway latency to obtain cocaine, compared with vehicle-treated rats. ***D***, Average ± SEM latency to reach the goal box of the last four trials. ** indicates $p < 0.01$, *** indicates $p < 0.01$(unpaired *t* test or ANOVA, respectively).

In the current study we observed several phenomena consistent with stronger RMTg activation by cocaine in high than low avoiders. These include (1) increased excitation by depolarizing current steps in high-avoiders, (2) increased presynaptic glutamatergic release onto the RMTg in high avoiders, and (3) reduced postsynaptic CP-AMPA receptors in low avoiders. Although the mechanisms underlying these observations are not fully understood, changes in CP-AMPA receptors are likely one possibility, as we observed marked differences in sensitivity of eEPSCs to NASPM between low and high avoiders. These findings led us to posit that low-avoider rats exhibit a downregulation of receptors lacking GluA2 subunits (and hence calcium permeable). However, mechanisms of our other observations are less clear. For example, we observed increased intrinsic excitability by depolarizing current steps in high avoiders versus both low avoiders and saline controls. Although CP-AMPAR levels are likely higher in high avoiders than low avoiders, we did not find evidence that they were higher than saline controls, suggesting that the differences in intrinsic excitability are because of changes in other membrane channels besides CP-AMPAR receptors. Finally, alterations in presynaptic release have often been attributed to retrograde signaling mechanisms (Arancio et al., 1996; Haj-Dahmane et al., 2017), and preliminary work in our lab supports this possibility, but again more work is needed to investigate this possibility.

Another major unresolved question arising from this work is whether the observed differences between low- and high-avoider rats are preexisting or arise in response to cocaine exposure. This is difficult to fully answer in outbred SD rats, as whole-cell measurements before cocaine exposure could be correlated with behavioral phenotype because of the need to kill the animal to obtain these recordings. Nonetheless the preponderance of our evidence suggests that synaptic differences emerge in response to cocaine. For example, when we patched RMTg neurons in cocaine-naive rats, we initially expected them to show a bimodal

distribution of synaptic properties, reflecting their as yet unrevealed bimodal behavioral phenotypes. Surprisingly, this was not the case, and instead, we saw that presynaptic properties were uniformly depotentiated, exhibiting high PPRs (reflecting low presynaptic release probabilities) similarly to low-avoider rats. In contrast, postsynaptic properties were uniformly potentiated in drug-naive rats, showing high AMPA/NMDA ratios, slow EPSC decay, and high sensitivity to NASPM, all consistent with high levels of CP-AMPAR signaling, similarly to high-avoider rats. These results suggest that cocaine exposure selectively upregulates presynaptic signaling in high-avoider rats but selectively downregulates postsynaptic signaling in low-avoider rats. In other words, the observed synaptic properties of RMTg neurons in the cocaine-naive condition do not resemble those of either low or high avoiders (nor a mixture of the two) but instead represent a third state that is altered after cocaine exposure.

Our findings suggest a number of questions to be addressed in future work. We found evidence that differing synaptic characteristics of high versus low avoiders only emerge after cocaine exposure, but it is not known why different animals respond so differently to cocaine nor whether these responses are because of differing predisposing genetic or environmental factors. Our current study also examined differential RMTg sensitivity to glutamatergic input but used a nonspecific electrical stimulation, which did not distinguish among the many possible glutamatergic inputs to the RMTg. We hypothesize a major contributor is the LHb, as it provides the single largest input to RMTg, and its neurons exhibit c-*fos* activation by cocaine, unlike other inputs that largely lack such activation (Jhou et al., 2013; TC Jhou, H Li, and Y Chao, unpublished observations). However, this remains to be tested. In the current study, we also did not attempt to investigate possible differences in LHb responses to cocaine because of the lack of difference in LHb c-*fos* responses to cocaine after seven runway trials. However, we cannot rule out that such differences could have occurred earlier as prior work has reported such transient adaptive changes in the LHb (Meye et al., 2015, 2016).

Finally, the current study raises the question of why high and low avoiders of cocaine do not differ on other aversion-related tasks such as elevated plus maze and shock-induced punishment (e.g., Fig. 1*E*,*F*), although the RMTg is critically required for both tasks (Jhou et al., 2009; Kaufling et al., 2009; Vento et al., 2017). One possibility is that different types of aversion-related stimuli activate the RMTg via distinct afferent pathways (Li et al., 2019b), suggesting the possibility that distinct aversive stimuli may be independently modulated via distinct neural pathways. However, this is still an area of active investigation.

In summary, we found that VTA-projecting RMTg neurons exhibit multiple functional differences that correlate with cocaine avoidance phenotypes and reflect cocaine-evoked plasticity. These differences might critically influence aversion to cocaine and hence addiction vulnerability, and further study is needed to identify the causative factors determining why different individuals exhibit such different behavioral and physiological responses.

References

Arancio O, Lev-Ram V, Tsien RY, Kandel ER, Hawkins RD (1996) Nitric oxide acts as a retrograde messenger during long-term potentiation in cultured hippocampal neurons. J Physiol Paris 90:321–322.

Bowie D, Mayer ML (1995) Inward rectification of both AMPA and kainate subtype glutamate receptors generated by polyamine-mediated ion channel block. Neuron 15:453–462.

Bowie D, Lange GD, Mayer ML (1998) Activity-dependent modulation of glutamate receptors by polyamines. J Neurosci 18:8175–8185.

Clem RL, Huganir RL (2010) Calcium-permeable AMPA receptor dynamics mediate fear memory erasure. Science 330:1108–1112.

Crepel F, Daniel H (2007) Developmental changes in agonist-induced retrograde signaling at parallel fiber-Purkinje cell synapses: role of calcium-induced calcium release. J Neurophysiol 98:2550–2565.

Crépel F, Galante M, Habbas S, McLean H, Daniel H (2011) Role of the vesicular transporter VGLUT3 in retrograde release of glutamate by cerebellar Purkinje cells. J Neurophysiol 105:1023–1032.

Davis CM, Riley AL (2010) Conditioned taste aversion learning: implications for animal models of drug abuse. Ann N Y Acad Sci 1187:247–275.

Deroche-Gamonet V, Belin D, Piazza PV (2004) Evidence for addiction-like behavior in the rat. Science 305:1014–1017.

Ellenbroek BA, van der Kam EL, van der Elst MC, Cools AR (2005) Individual differences in drug dependence in rats: the role of genetic factors and life events. Eur J Pharmacol 526:251–258.

Erlenhardt N, Yu H, Abiraman K, Yamasaki T, Wadiche JI, Tomita S, Bredt DS (2016) Porcupine controls hippocampal AMPAR levels, composition, and synaptic transmission. Cell Rep 14:782–794.

Ettenberg A (2009) The runway model of drug self-administration. Pharmacol Biochem Behav 91:271–277.

Ettenberg A, Raven MA, Danluck DA, Necessary BD (1999) Evidence for opponent-process actions of intravenous cocaine. Pharmacol Biochem Behav 64:507–512.

Ettenberg A, Fomenko V, Kaganovsky K, Shelton K, Wenzel JM (2015) On the positive and negative affective responses to cocaine and their relation to drug self-administration in rats. Psychopharmacology (Berl) 232:2363–2375.

Fowler CD, Kenny PJ (2014) Nicotine aversion: neurobiological mechanisms and relevance to tobacco dependence vulnerability. Neuropharmacology 76 Pt B:533–544.

Gao P, Groenewegen HJ, Vanderschuren L, Voorn P (2018) Heterogeneous neuronal activity in the lateral habenula after short- and long-term cocaine self-administration in rats. Eur J Neurosci 47:83–94.

Haj-Dahmane S, Bëique JC, Shen R-Y (2017) GluA2-lacking AMPA receptors and nitric oxide signaling gate spike-timing-dependent potentiation of glutamate synapses in the dorsal raphe nucleus. eNeuro 4: ENEURO.0116-17.2017.

Isaac JT, Ashby MC, McBain CJ (2007) The role of the GluR2 subunit in AMPA receptor function and synaptic plasticity. Neuron 54:859–871.

Jhou TC, Good CH, Rowley CS, Xu SP, Wang H, Burnham NW, Hoffman AF, Lupica CR, Ikemoto S (2013) Cocaine drives aversive conditioning via delayed activation of dopamine-responsive habenular and midbrain pathways. J Neurosci 33:7501–7512.

Jhou TC, Fields HL, Baxter MG, Saper CB, Holland PC (2009) The rostromedial tegmental nucleus (RMTg), a GABAergic afferent to midbrain dopamine neurons, encodes aversive stimuli and inhibits motor responses. Neuron 61:786–800.

Jonas P, Burnashev N (1995) Molecular mechanisms controlling calcium entry through AMPA-type glutamate receptor channels. Neuron 15:987–990.

Kaufling J, Veinante P, Pawlowski SA, Freund-Mercier MJ, Barrot M (2009) Afferents to the GABAergic tail of the ventral tegmental area in the rat. J Comp Neurol 513:597–621.

Knackstedt LA, Samimi MM, Ettenberg A (2002) Evidence for opponent-process actions of intravenous cocaine and cocaethylene. Pharmacol Biochem Behav 72:931–936.

Koob GF (2006) The neurobiology of addiction: a neuroadaptational view relevant for diagnosis. Addiction 101:23–30.

Koob GF, Le Moal M (2008) Review. Neurobiological mechanisms for opponent motivational processes in addiction. Philos Trans R Soc Lond B Biol Sci 363:3113–3123.

Kreitzer AC, Malenka RC (2005) Dopamine modulation of state-dependent endocannabinoid release and long-term depression in the striatum. J Neurosci 25:10537–10545.

Kreitzer AC, Regehr WG (2001) Retrograde inhibition of presynaptic calcium influx by endogenous cannabinoids at excitatory synapses onto Purkinje cells. Neuron 29:717–727.

Lecca S, Melis M, Luchicchi A, Ennas MG, Castelli MP, Muntoni AL, Pistis M (2011) Effects of drugs of abuse on putative rostromedial tegmental neurons, inhibitory afferents to midbrain dopamine cells. Neuropsychopharmacology 36:589–602.

Lecca S, Melis M, Luchicchi A, Muntoni AL, Pistis M (2012) Inhibitory inputs from rostromedial tegmental neurons regulate spontaneous

activity of midbrain dopamine cells and their responses to drugs of abuse. Neuropsychopharmacology 37:1164–1176.

Li H, Pullmann D, Cho JY, Eid M, Jhou TC (2019a) Generality and opponency of rostromedial tegmental (RMTg) roles in valence processing. eLife 8:e41542.

Li H, Vento PJ, Parrilla-Carrero J, Pullmann D, Chao YS, Eid M, Jhou TC (2019b) Three rostromedial tegmental afferents drive triply dissociable aspects of punishment learning and aversive valence encoding. Neuron 104:987–999.e4.

Li H, Eid M, Pullmann D, Chao YS, Thomas AA, Jhou TC (2020) Entopeduncular nucleus projections to the lateral habenula contribute to cocaine avoidance. J Neurosci 41:298–306.

Liu SJ, Zukin RS (2007) Ca2+-permeable AMPA receptors in synaptic plasticity and neuronal death. Trends Neurosci 30:126–134.

Malinow R, Malenka RC (2002) AMPA receptor trafficking and synaptic plasticity. Annu Rev Neurosci 25:103–126.

Maroteaux M, Mameli M (2012) Cocaine evokes projection-specific synaptic plasticity of lateral habenula neurons. J Neurosci 32:12641–12646.

Meye FJ, Valentinova K, Lecca S, Marion-Poll L, Maroteaux MJ, Musardo S, Moutkine I, Gardoni F, Huganir RL, Georges F, Mameli M (2015) Cocaine-evoked negative symptoms require AMPA receptor trafficking in the lateral habenula. Nat Neurosci 18:376–378.

Meye FJ, Soiza-Reilly M, Smit T, Diana MA, Schwarz MK, Mameli M (2016) Shifted pallidal co-release of GABA and glutamate in habenula drives cocaine withdrawal and relapse. Nat Neurosci 19:1019–1024.

Ohno-Shosaku T, Tsubokawa H, Mizushima I, Yoneda N, Zimmer A, Kano M (2002) Presynaptic cannabinoid sensitivity is a major determinant of depolarization-induced retrograde suppression at hippocampal synapses. J Neurosci 22:3864–3872.

Piazza PV, Deroche-Gamonet V (2013) A multistep general theory of transition to addiction. Psychopharmacology (Berl) 229:387–413.

Proulx CD, Aronson S, Milivojevic D, Molina C, Loi A, Monk B, Shabel SJ, Malinow R (2018) A neural pathway controlling motivation to exert effort. Proc Natl Acad Sci U S A 115:5792–5797.

Riley AL (2011) The paradox of drug taking: the role of the aversive effects of drugs. Physiol Behav 103:69–78.

Sánchez-Catalán MJ, Faivre F, Yalcin I, Muller MA, Massotte D, Majchrzak M, Barrot M (2016) Response of the tail of the ventral tegmental area to aversive stimuli. Neuropsychopharmacology 42:638–648.

Smith RJ, Vento PJ, Chao YS, Good CH, Jhou TC (2019) Gene expression and neurochemical characterization of the rostromedial tegmental nucleus (RMTg) in rats and mice. Brain Struct Funct 224:219–238.

Stamatakis AM, Stuber GD (2012) Activation of lateral habenula inputs to the ventral midbrain promotes behavioral avoidance. Nat Neurosci 15:1105–1107.

Stincic TL, Frerking ME (2015) Different AMPA receptor subtypes mediate the distinct kinetic components of a biphasic EPSC in hippocampal interneurons. Front Synaptic Neurosci 7:7.

Swanson GT, Kamboj SK, Cull-Candy SG (1997) Single-channel properties of recombinant AMPA receptors depend on RNA editing, splice variation, and subunit composition. J Neurosci 17:58–69.

Sweitzer MM, Donny EC, Hariri AR (2012) Imaging genetics and the neurobiological basis of individual differences in vulnerability to addiction. Drug Alcohol Depend 123 Suppl 1:S59–S71.

Ting JT, Daigle TL, Chen Q, Feng G (2014) Acute brain slice methods for adult and aging animals: application of targeted patch clamp analysis and optogenetics. Methods Mol Biol 1183:221–242.

Tsuang MT, Lyons MJ, Meyer JM, Doyle T, Eisen SA, Goldberg J, True W, Lin N, Toomey R, Eaves L (1998) Co-occurrence of abuse of different drugs in men: the role of drug-specific and shared vulnerabilities. Arch Gen Psychiatry 55:967–972.

Uhl GR (2004) Molecular genetic underpinnings of human substance abuse vulnerability: likely contributions to understanding addiction as a mnemonic process. Neuropharmacology 47:140–147.

Van Etten ML, Anthony JC (1999) Comparative epidemiology of initial drug opportunities and transitions to first use: marijuana, cocaine, hallucinogens and heroin. Drug Alcohol Depend 54:117–125.

Vento PJ, Burnham NW, Rowley CS, Jhou TC (2017) Learning from one's mistakes: a dual role for the rostromedial tegmental nucleus in the encoding and expression of punished reward seeking. Biol Psychiatry 81:1041–1049.

Verdoorn TA, Burnashev N, Monyer H, Seeburg PH, Sakmann B (1991) Structural determinants of ion flow through recombinant glutamate receptor channels. Science 252:1715–1718.

Wang Q, Li D, Bubula N, Campioni MR, McGehee DS, Vezina P (2017) Sensitizing exposure to amphetamine increases AMPA receptor phosphorylation without increasing cell surface expression in the rat nucleus accumbens. Neuropharmacology 117:328–337.

Wheeler DS, Robble MA, Hebron EM, Dupont MJ, Ebben AL, Wheeler RA (2015) Drug predictive cues activate aversion-sensitive striatal neurons that encode drug seeking. J Neurosci 35:7215–7225.

Wheeler RA, Twining RC, Jones JL, Slater JM, Grigson PS, Carelli RM (2008) Behavioral and electrophysiological indices of negative affect predict cocaine self-administration. Neuron 57:774–785.

Wilson RI, Nicoll RA (2001) Endogenous cannabinoids mediate retrograde signalling at hippocampal synapses. Nature 410:588–592.